Jurnal Tribologi 47 (2025) 87-103

MYTRIBOS Malaysian Tribology Society

Jurnal Tribologi

Website : jurnaltribologi.mytribos.org e-issn: 2289-7232

Tribological characteristics using TiC nanoparticles as surface reinforcement on duplex stainless steel

Alin Qistina Shamsuri [1], Lailatul Hairina Paijan [1*], Zulkifli Mohd Rosli [1], Jainuddin Ibrahim [1], Ahmed Nazrin Md Idriss [2], Aslam Hadi Hamzah [3]

[1] Faculty of Industrial and Manufacturing Technology and Engineering, Universiti Teknikal Malaysia Melaka, MALAYSIA.
[2] College of Engineering, Universiti Teknologi MARA, MALAYSIA.
[3] ORS Technologies Sdn Bhd, MALAYSIA.
*Corresponding author: lailatulharina@utem.edu.my

KEYWORDS

Tribological
Nanoparticles
Arcing current
Pulse frequency
TIG melting
Wear

ABSTRACT

This study focused on the surface modification of duplex stainless steel (DSS) through the deposition of 10 nm titanium carbide (TiC) nanoparticles using the tungsten inert gas (TIG) melting technique, aimed at enhancing the material's wear resistance. Despite the inherent advantages of DSS, its wear resistance in abrasive environments posed significant challenges for various engineering applications, necessitating innovative solutions to improve its durability. The primary objective is to produce a composite coating layer on DSS, characterize its properties, and evaluate its hardness and wear resistance. The methodology involved TIG parameters using arcing currents from 120 A to 140 A with a different pulse frequency ranging between 15, 20 and 25 pulse per second (PPS). The thickness layer, micrograph, microhardness profile and wear performance of composite coatings were conducted using Field Emission Scanning Electron Microscopy (FE-SEM), Vickers microhardness tester and reciprocating wear test, respectively. Wear track analysis included 3D surface topography, wear depth, and mechanism. The key results indicated that the incorporation of TiC nanoparticles significantly improved the hardness and wear properties of DSS due to the high population of TiC nanoparticles and lesser wear depth. The optimal conditions, achieved at 140 A with 25 PPS, resulted in a thickness layer of 900 µm, maximum hardness of 394.3 Hv, a coefficient of friction of 0.08, and a wear depth of 81.34 µm.

Received 22 June 2025; received in revised form 10 August 2025; accepted 3 September 2025.
To cite this article: Shamsuri et al. (2025). Tribological characteristics using TiC nanoparticles as surface reinforcement on duplex stainless steel. Jurnal Tribologi 47, pp.87-103.

1.0 INTRODUCTION

Duplex stainless steel was characterized by its unique microstructure, which combined both austenitic and ferritic phases, providing enhanced strength and corrosion resistance. It had been widely utilized in various industries due to its favorable mechanical properties and resistance to stress corrosion cracking, making it suitable for demanding applications (Islam & Rashed., 2019). However, DSS shows certain weaknesses in terms of hardness and wear resistance, which restricts its application in many tribological circumstances (Paijan et al., 2022). Therefore, it is necessary to modify the surface of the material by depositing ceramic particles as a potential technique to enhance the hardness and reduce the wear problem (Maleque & Afiq., 2018). Furthermore, in a study from Paijan & Maleque (2018) employed DSS as a surface coating to improve tribological properties through the deposition of silicon carbide (SiC) ceramic particles. The results indicate that the coated surface exhibited a significant improvement, with reduced wear weight loss and a coefficient of friction approximately two times lower than that of the substrate material. The incorporation of SiC into the surface of steel has enhanced the wear characteristics of DSS.

Tungsten Inert Gas (TIG) welding is a highly reliable and adaptable method of joining metals. This approach uses an inert gas, like argon or helium, to protect the weld area from air contamination, it uses a non-consumable tungsten electrode to create the weld. The ability of TIG welding to create excellent, clean welds on a range of metals (Azevedo & Resende, 2021; Paijan et al., 2023). According to Shi et al. (2020), a substrate's surface can be coated with TIG torch cladding to make it resistant to wear and corrosion. This is particularly helpful for parts that wear out quickly, such as compressors, industrial machinery, and valves. A substrate's service life can be significantly extended by depositing materials that are more resistant to erosion or corrosion.

TiC is a ceramic material distinguished by its high melting point, exceptional hardness, and excellent conductivity. It is commonly used to strengthen and extend the life of cutting tools, wear-resistant coatings, and metal matrix composites. A study by Chi et al. (2021), investigated the in-situ Titanium Diboride–Titanium Carbide (TiB_2–TiC) reinforced Iron-Aluminum (Fe-Al) composite coating on 6061 grade aluminum alloy by laser surface modification. In the result, the average micro-hardness increased, more than 7 times higher than the substrate material. Meanwhile, a notable improvement in wear resistance was indicated by a 92.8% decrease in volume loss. Other studies by Sun et al. (2022) investigated the application of TiC powder sizes ranging from 2 to 4 μm for surface modification onto Molybdenum Iron Boride (Mo_2FeB_2) alloy substrates via TIG cladding techniques. The findings indicated a noteworthy enrichment in the mechanical characteristics of the composite coating layers, with hardness values reaching 1035 Hv for the 5% TiC content. In the meantime, wear resistance exhibits 14.6 times higher than that of the substrate material.

According to the literature, incorporating TiC ceramic particulates using the powder pre-replacement method and melting under a TIG torch could be a significant advancement in surface modification. This research provides a unique perspective on using TiC nanoparticles and the conventional TIG technique for composite coating layers, offering a cost-effective alternative to fusion processes. Previous studies have shown that surface modifications via TIG torch melting with TiC nanoparticles effectively enhance the surface coating of various substrate materials in terms of surface hardness and wear properties. However, previous research has mainly focused on different ceramic particles and substrate materials, neglecting the incorporation of TiC nanoparticles into the hard facing of DSS using the TIG torch melting process. This study aims to address this gap by incorporating TiC nanoparticles with varying current and pulse frequencies

on DSS surfaces. Investigating the formation of composite coating layers on DSS is expected to significantly improve surface hardness and wear resistance. Additionally, it is crucial to consider process parameters, as they play a crucial role in the composite coating layer of DSS.

2.0 EXPERIMENTAL PROCEDURE

Alloy 2205 duplex stainless steel with dimensions of 50 × 30 × 10 mm was used as a substrate in this work, and its chemical compositions are displayed in Table 1 (Kısasöz et al., 2017). Subsequently, the substrate surface underwent abrasive grinding with sandpaper ranging from 60 to 240. The surface was thoroughly cleaned with ethanol to remove contaminants such as oil and grease. In order to produce the composite coating, TiC nanoparticles with particle sizes of 10 nm were pre-placed on the surface of the substrate. The nanoparticles mixture weighed of 0.5 mg/mm^2 were mixed with two drops of ethanol, two drop of distilled water and two drop of polyvinyl acetate (PVA) to form a paste. The purpose of the PVA addition is to act as a binder, ensuring that the TiC paste stays to the substrate's surface while the shielding gas flows during the TIG melting technique. Finally, the pre-placed samples were dried in an oven at 80oC for 1 hour to remove any residual moisture from the TiC paste.

Table 1: Elemental chemical composition of 2205 DSS.

Type	C	Cr	Si	Mo	Mn	S	Fe
2205 DSS	0.026	22.06	0.69	2.58	1.74	0.008	Balance

A TIG welding machine was used to produce the composite coating with arcing currents of 120 A and 140 A and varying pulse frequencies of 15, 20, and 25 PPS. This investigation aimed to determine the impact of these parameters on the microstructural and wear properties of DSS. During the melting process, 15 L/min argon gas is used as a shielding gas to prevent excessive oxidation of the molten pool. Figure 1 shows the workflow diagram for TIG melting using TiC nanoparticles deposited on DSS surface. Meanwhile, the 50% overlapping technique was applied to cover the whole surface of DSS to form a composite coating, as shown in Figure 2. The TIG melting technique parameters used in the composite coating development are depicted in Table 2.

After TIG melting techniques, the coated substrate was cleaned to remove any excess bonded powders and subsequently cut into cross-sections using an Electrical Discharge Machining (EDM) wire-cutting process. The cross-section sample was subsequently ground and polished using sandpaper with grit sizes of 60, 240, 300, 400, 600, 800, and 1200, followed by cloth polishing with an alumina suspension until mirror finishes. Then, etched with Kalling's reagent to expose the microstructure. The thickness layer of composite coating was measured using Leica Digital Microscope with 100 μm magnification. The micrograph analysis of the cross-sectional sample was conducted using FE-SEM at 3000X magnification. Meanwhile, a Vickers microhardness tester was used with a force load of 0.5 kgf and a 10-second indentation time to measure the hardness profile along the depth penetration of the composite coating DSS. For wear testing, a ball-on-disc tribometer was utilized against a 6 mm alumina ceramic ball, with the test conditions displayed in Table 3. Subsequently, the 3S surface topography and wear scars were evaluated using digital microscope and FESEM, respectively.

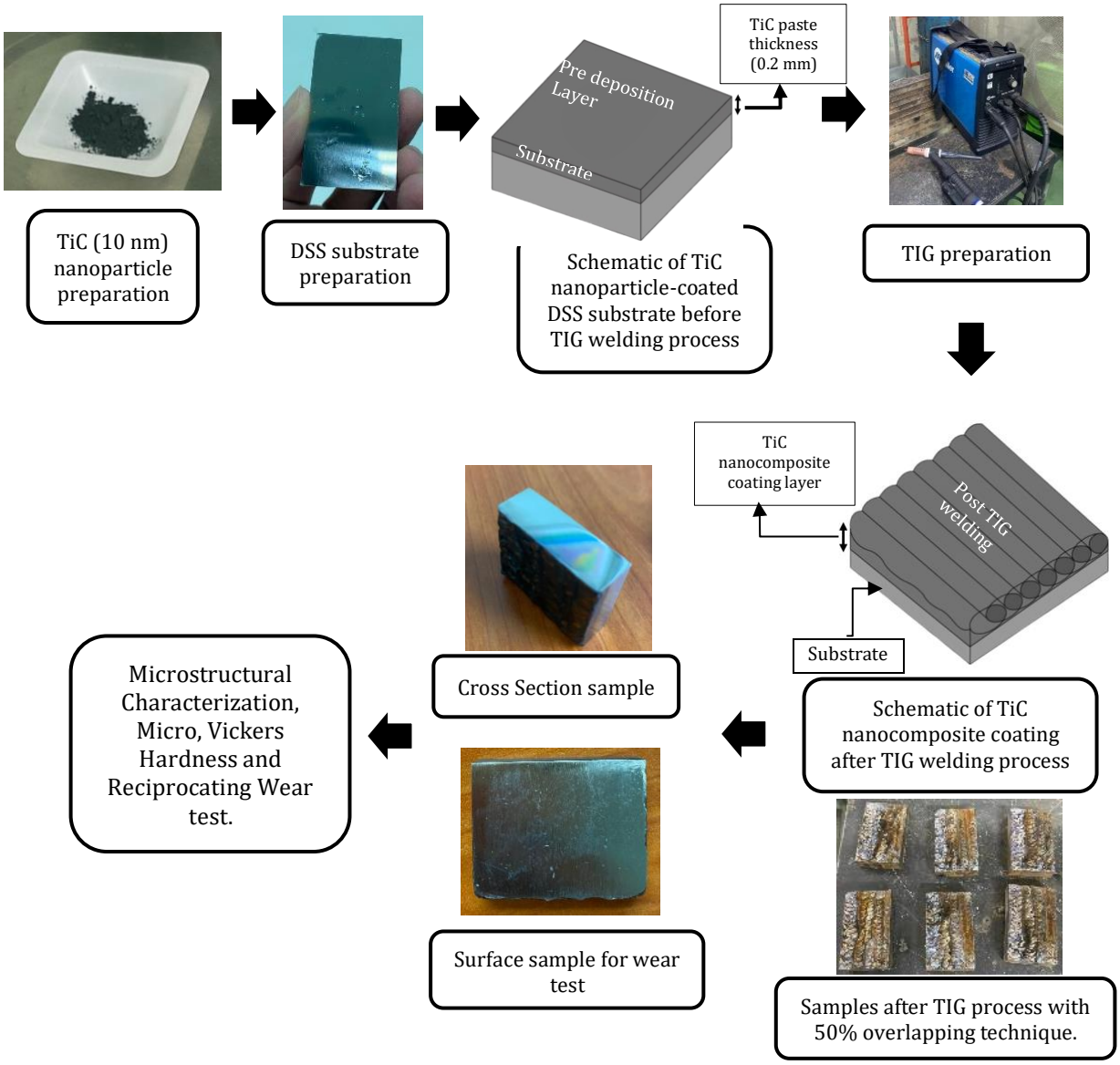

Figure 1: Workflow diagram for TIG melting using TiC 10 nm ceramic particles deposited on DSS surface.

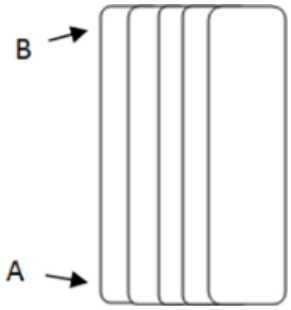

Figure 2: Illustrations of 50% overlapping tracks of multi-pass welds. (A) signified as initiating point for producing the multi-pass layer to the end of point (B) where melting stops.

Table 2: TIG arcing parameters used in the composite coating layer of DSS.

Experiment no.	Current (Amperage-A)	Pulsed Frequency (pulse/second - PPS)
1	120	15
2		20
3		25
4	140	15
5		20
6		25

Table 3: Wear test condition.

Specimen	Reciprocating wear test conditions for linear motion
Applied load	20 N
Frequency	15 Hz
Wear test duration	15 minutes
Counter-part body	Alumina ceramic ball 6 mm
Stroke Length	15 mm
Sliding Distance	406 m
Sliding Speed	300 revolutions per minute (rpm)

3.0 RESULTS AND DISCUSSION

3.1 Thickness Layer and Micrograph of TiC Nano-Composite Coating

The cross-section of the thickness layer and micrograph of TiC nanocomposite coating examined under a digital microscope and FE-SEM equipment are shown in Figures 3(a-f). Meanwhile, the graph comparison for the thickness layer using different currents and pulse frequencies is depicted in Table 4. The effect of arcing currents on the substrate significantly influences the thickness layer and micrograph of the composite coating, particularly on the distribution of TiC nanoparticles within the layer.

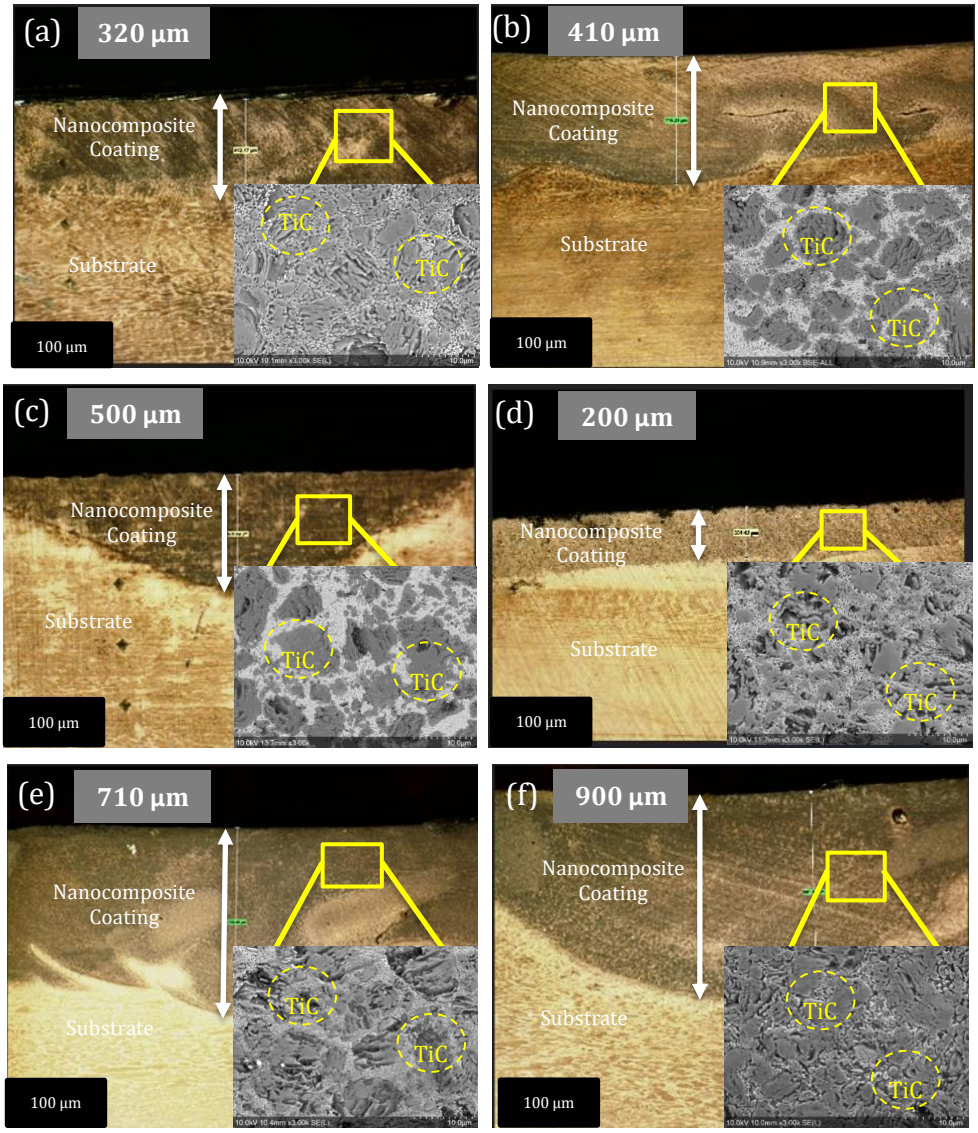

Figure 3: Thickness layer and FESEM micrographs (×3,000 magnification) of TiC nano-composite coating using different TIG process parameters; (a) 120 A 15 PPS, (b) 120 A 20 PPS, (c) 120 A 25 PPS, (d) 140 A 15 PPS, (e) 140 A 20 PPS and (d) 140 A 25 PPS.

Table 4 shows that as the pulse frequencies increase from 15 to 25 PPS with 120 A current, the thickness layer increases from 320 to 500 µm as shown in Figures 3(a-c) due to higher pulse frequencies, which helps to control the amount of heat being applied, leading to a more controlled and consistent deposition of TiC nanoparticles into the surface layer. However, the thickness of layer drops (200 µm) at 140 A current and 15 PPS (Figure 3d) owing to excessive heat input, which reduces the overall deposition efficiency. Furthermore, when the pulse increases from 20 to 25 PPS, the thickness of the layer increases again from 710 µm to 900 µm as shown in Figures 3 (e & f) due to improved heat distribution and reduced heat accumulation. This shows that the

higher current and pulse frequencies focus the arc energy, creating a more intense and localized heat zone. This enhances the melting of the DSS, improves the integration of ceramic particles into the surface, and ensures that the particles are embedded deeper and more uniformly. It can also be observed from the micrograph that the spherical TiC shape is large and dispersed well in the sample.

Table 4: Thickness composite coating layer using different currents and pulse frequencies of TiC nano-composite coating.

Exp. No.	Current (Amperage-A)	Pulsed Frequency (pulse/second - PPS)	Thickness coating layer (μm)
1	120	15	320
2		20	410
3		25	500
4	140	15	200
5		20	710
6		25	900

In contrast, Figure 3(d) shows the lowest thickness layer of 200 μm occurring at 140 A and 15 PPS. This phenomenon might be due to lower pulse frequencies distributing energy in shorter bursts, minimizing overall heat buildup and reducing deposition efficiency, which produced a thinner layer. Based on the micrograph, this sample also produces the reduction of TiC nanoparticle dispersion, which promotes the lower population in the composite coating. The lower pulse frequencies reduce the intensity and dynamics of the welding process, leading to insufficient melting and shallower penetration. Thus, it produces a poor distribution, less bonding of ceramic particles, inconsistent deposition and finally reduces the thickness layer of the composite coating. Ardeshir et al., (2024), observed that coating thickness increased when AlNiCoCrFe powder was added to plain carbon steel using the TIG melting process. The study found that higher welding currents resulted in thicker coatings. Specifically, the depth of the molten layer significantly increased from 192 to 1862 μm as the current was increased from 90 to 130 A.

3.2 Micro-Hardness Profile for TiC Composite Coating

To further understand the impact of microstructural properties on the performance of the composite coating DSS, the microhardness profile measurements were performed at the cross-section samples with different regions from the upper surface to the substrate region, as presented in Figure 4. The microhardness profile shows a gradual decline from the upper surface of the composite coating DSS to the substrate region. This can be linked to the slow cooling rate of DSS. Figure 5 illustrates the variation in micro-Vickers hardness for top surface of TiC nano-composite coatings under different TIG process parameters, with error bars indicating the consistency and reliability of the measurements. As the currents and pulse frequencies increase, the TiC nanoparticles tend to migrate deeper into the material, leaving the surface layer highly reinforced with the ceramic particle deposition.

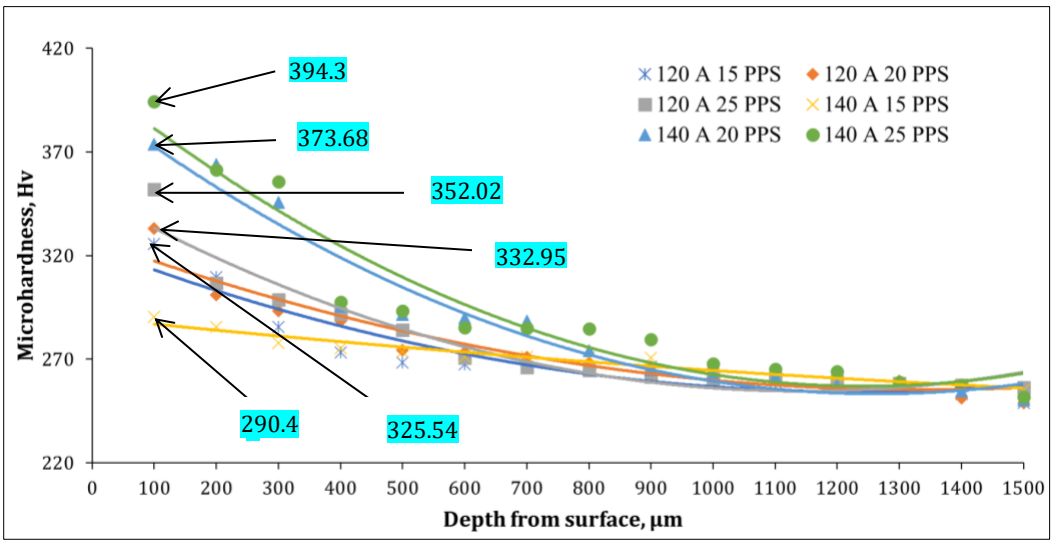

Figure 4: Microhardness profile of TiC nano-composite coating using different TIG current and pulse frequencies.

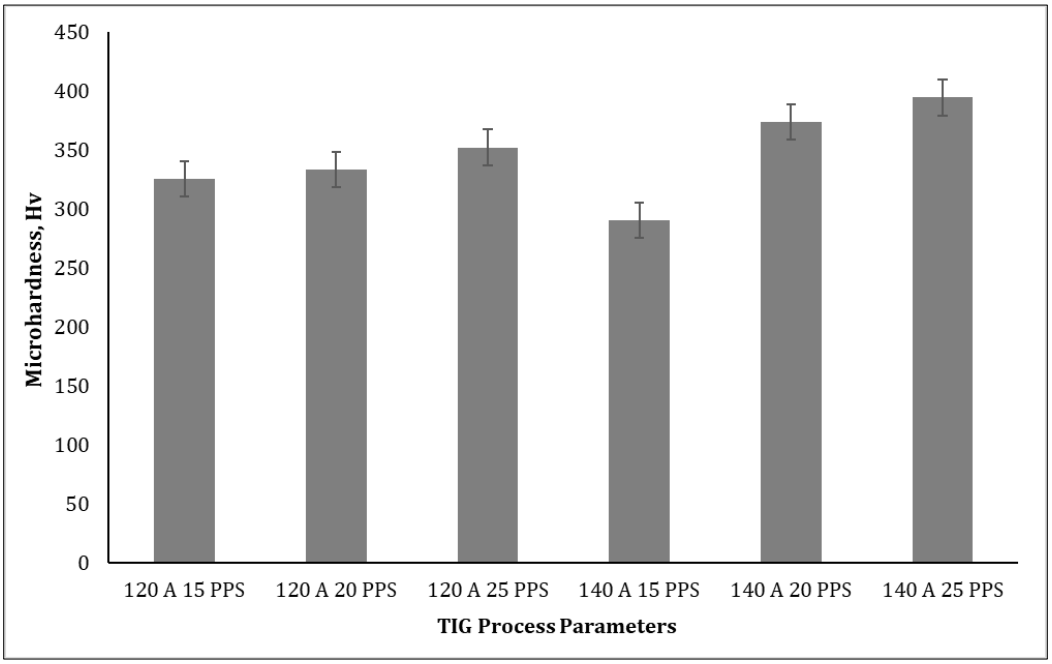

Figure 5: Micro-Vickers top surface hardness values of TiC nanocomposite coatings under different TIG process parameters. Error bars represent standard deviation.

Furthermore, at 120 A current, the hardness improved by 8.42% from 325.54 Hv to 352.95 Hv as the pulse frequencies increased from 15 to 25 PPS. This is due to the enhanced dispersion and bonding of TiC nanoparticles at higher pulse frequencies, which creates a more homogeneous and

harder surface layer with a higher population of TiC nanoparticles as shown in Figures 3(a-c). Conversely, at 140 A and 15 PPS, the hardness suddenly decreased to 290.48 Hv due to excessive heat from the high current, which weakened the composite coating. The high current reduced the effectiveness of the TiC nanoparticles, which are supposed to make the material harder and stronger. As a result, the surface layer became softer and less durable. However, when the pulse frequencies were raised from 20 to 25 PPS processed at 140 A, the hardness increased by 5.52% from 373.68 Hv to 394.30 Hv. This enhancement is due to the optimal combination of high current and higher pulse frequencies, which provided sufficient energy input, enhancing the bonding and distribution of TiC nanoparticles. This leads to a more reinforced and harder surface with a greater population of TiC nanoparticles.

This trend highlights that while the condition at 140 A and 15 PPS presented challenges due to excessive heat input and poor TiC nanoparticle dispersion, adjusting the pulse frequencies to higher levels significantly reduced these issues and resulted in enhanced microstructural properties and hardness at 140 A and 25 PPS. The result obtained agreed with previous work carried out by Paraye et al., (2021), which studied in-situ grown TiC-reinforced steel matrix produced with TIG arcing by the metallurgical reaction between titanium and graphite powder on bearing steel (AISI 8620). The average hardness of the modified surface reached about 2.15 times that of the base metal. It is noticed that with the rise in current from 80 to 140 and 200 A, the depth of the fusion zone enhances from 1.3 to 2.45 and 3.05 mm, respectively. Thus, in the presence of precipitate and the martensite matrix, the microhardness of the surface composite improved significantly from 242 HV (base) to 522 HV for the sample processed with 200 A. Other research conducted by Maleque et al., (2024), investigates TiC particulates incorporated on the surface of the AISI 4340 grade steel at different content and heat inputs using the TIG melting process. The TiC content and heat input varied, with values ranging from 1008, 1296, and 2160 J/mm for various powder densities. The findings revealed that as the heat input increased to 2160 J/mm, the microhardness values increased significantly, reaching approximately 1050 HV, indicating that higher heat input leads to increased hardness. Higher heat input, combined with lower powder content, improved substrate and particulate dissolution.

The current research found that changing the current and pulse frequency had a significant effect on the microstructure of the TiC composite coating, which may influence its CoF properties as discussed in section 3.3. Higher pulse frequencies from 20 to 25 PPS resulted in more consistent energy input with refine and uniform distribution of TiC nanoparticles. This even particle distribution contributed to the coating's increased hardness and wear resistance. Lower pulse frequencies at 15 PPS resulted in less frequent energy input, causing the TiC nanoparticles to be larger and more unevenly distributed. The inconsistency in particle distribution had a negative impact on the coating's hardness and wear resistance. These findings indicate that optimizing pulse frequency is critical for achieving desired coating properties.

3.3 Coefficient of Friction (CoF) for TiC Nano-Composite Coating

The CoF was recorded during the reciprocating wear test on the DSS surface and plotted in Figure 6. At 120 A current, the CoF increased from 0.09 to 0.12 as the pulse frequencies increased from 15 to 20 PPS. This initial rise is due to an increase in surface roughness that elevated friction. Interestingly, at 120 A and 25 PPS, the CoF decreased to 0.11 because the surface became smoother, resulting in less friction. This smoother surface can be attributed to the optimal energy input during the TIG torch process, which refines the microstructure and reduces surface irregularities.

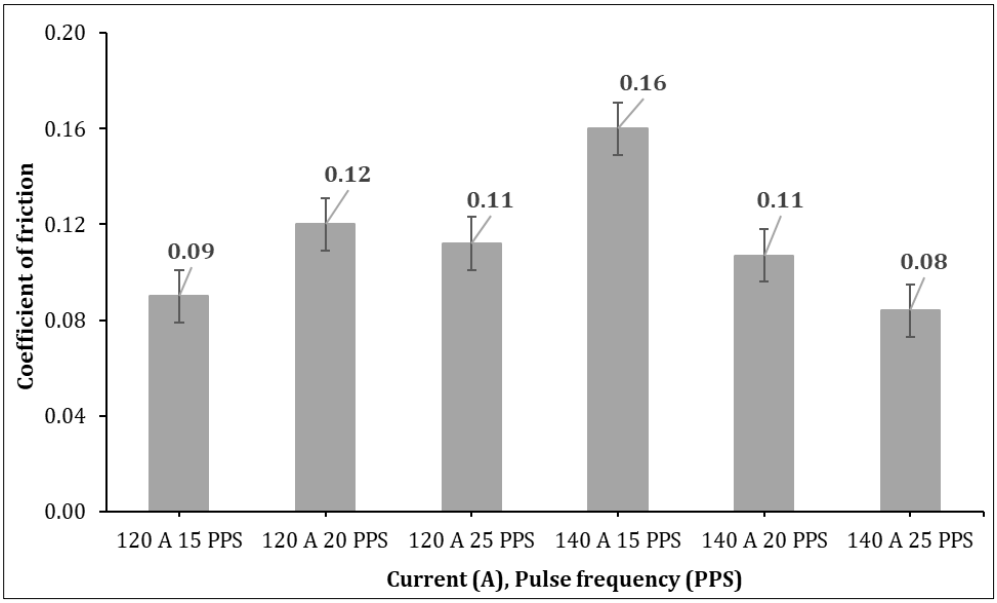

Figure 6: CoF of TiC nano-composite coating using different TIG current and pulse frequencies.

Subsequently, when the current reached 140 A, the CoF indicated a stabilized wear condition due to the consistent interaction between the composite coating and the counterpart material. This stability is achieved through a balanced formation and removal of wear debris and a stable surface layer that prevents excessive wear. The CoF ranged from 0.16 to 0.08 as pulse frequencies increased from 15 to 25 PPS, highlighting the effectiveness of this parameter in reducing friction. It may appear that at 15 PPS is owing to the rough surface created by less optimal energy input. As the pulse frequency increases, the energy input becomes more controlled, better dispersion of TiC nanoparticles, enhancing the hardness and wear resistance of the coating. This leads to a decrease in the CoF at higher frequencies like 20 and 25 PPS. Notably, the lowest CoF of 0.08 was observed for the TiC composite coating fabricated at 140 A and 25 PPS, indicating the optimal microstructure and surface characteristics achieved at this combination of current and pulse frequency. It is worth noting that the effect of increasing pulse frequency differs significantly between 120 A and 140 A. At 120 A, the arcing current may be insufficient to fully stabilize the melt pool, and increasing pulse frequency can lead to more rapid thermal cycling, which disrupts surface uniformity and increases friction. In contrast, at 140 A, the higher current provides sufficient energy to support deeper melting and better nanoparticle integration. The increasing pulse frequency enhances surface reflow and coating uniformity, resulting in a smoother surface and lower CoF. This contrast highlights the importance of pulse frequency with adequate current to achieve optimal CoF performance.

Overall, the higher current and pulse frequency not only improves the hardness and structural integrity of the coating but also enhances the interaction between the TiC nano-composite coating and the DSS surface, influencing its frictional behavior. Surface roughness analysis, as shown in Figure 7, supports the correlation between CoF and surface morphology. The lowest Ra value of 1.38 µm was recorded at 140 A and 25 PPS, which corresponds to the lowest CoF, indicating a smoother surface finish. This is similar to previous findings by Maleque et al., (2018) which demonstrated the enhancement of the tribological properties of titanium alloy grade 5 (Ti6Al-4V)

preplaced with SiC powder and then melted using TIG torch surface melting technique. The results showed that the lower CoF produced is related to the higher hardness value and higher distribution of carbides in the modified surface layer. As a result, the load transferred to the surface of the sample is reduced during wear sliding. Other research by Kumar & Das, (2021), examined the SiC-reinforced Cobalt (Co) coatings applied to AISI 304 steel using the TIG coating technique. The parameters varied were heat inputs of 432 J/mm, 480 J/mm, and 528 J/mm. The findings indicated that the COF for composite coatings significantly reduced and varied between 0.40 and 0.49 depending on the heat input, while the COF for AISI 304 steel remained at 0.51. Notably, the composite coating produced at 528 J/mm heat input exhibited the lowest COF of 0.40.

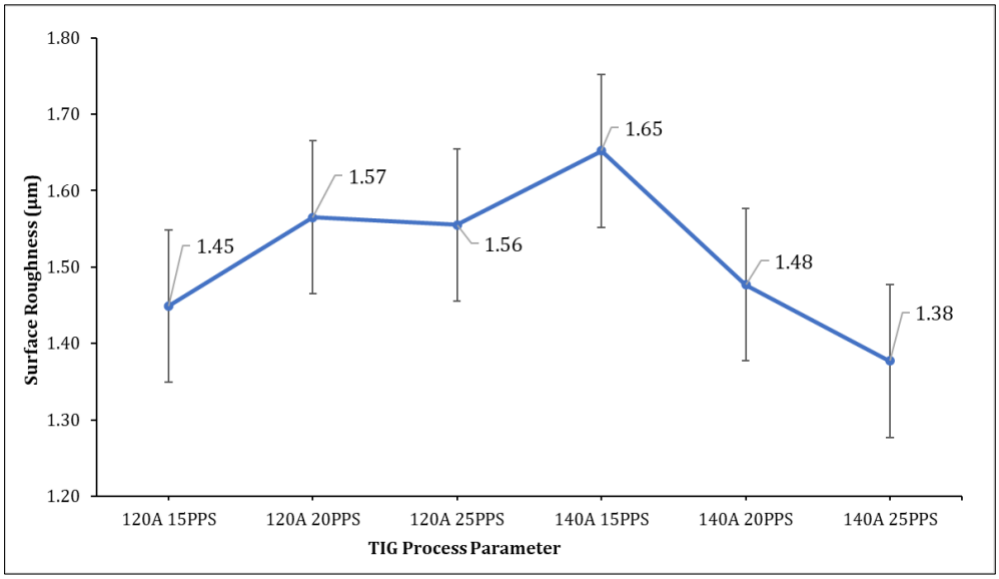

Figure 7: Surface roughness (Ra) values of TiC nanocomposite coatings under different TIG process parameters. Error bars represent standard deviation.

While the study shows significant improvements in DSS hardness and wear resistance due to the incorporation of TiC nanoparticles, certain limitations must be addressed. One potential limitation is the variability in coating thickness, which could affect the material's consistency. Achieving uniform dispersion of TiC nanoparticles across all samples proved difficult, potentially affecting the reliability of the results. Future research should concentrate on optimizing the TIG melting parameters to improve coating uniformity and reduce variability. Addressing these limitations will be critical for further optimizing the process and ensuring the validity of the results.

3.4 3D Surface Topography For TiC Nano-Composite Coating

Following the findings from the CoF analysis, the 3D surface topography images provide further insight into the wear performance of the TiC nanocomposite coating. The comprehensive analysis of the 3D surface topography images, using various TIG process parameters, is shown in Figures 8 (a-f). However, the topography image was not able to cover the entire wear depth due to magnification limitations of the equipment lens. The topography only covers half of the entire

wear depth for this analysis. In addition, the wear depth on the wear scars of nano-composite coating under different parameters is shown in Table 5.

Initially, based on Figure 8(a) at arcing currents of 120 A with 15 PPS, the wear depth was 87.32 µm, indicating a moderate level of wear depth with a reasonably consistent and smooth coating, offering decent wear resistance. However, increasing the pulse frequencies from 20 to 25 PPS (Figures 8b & 8c), resulted in a higher wear depth from 137.65 µm to 139.83 µm, representing a 53.1% increment of the wear penetration. This indicates a significant material loss and a rough surface, implying poorer wear resistance and reduced durability of the composite coating on this sample.

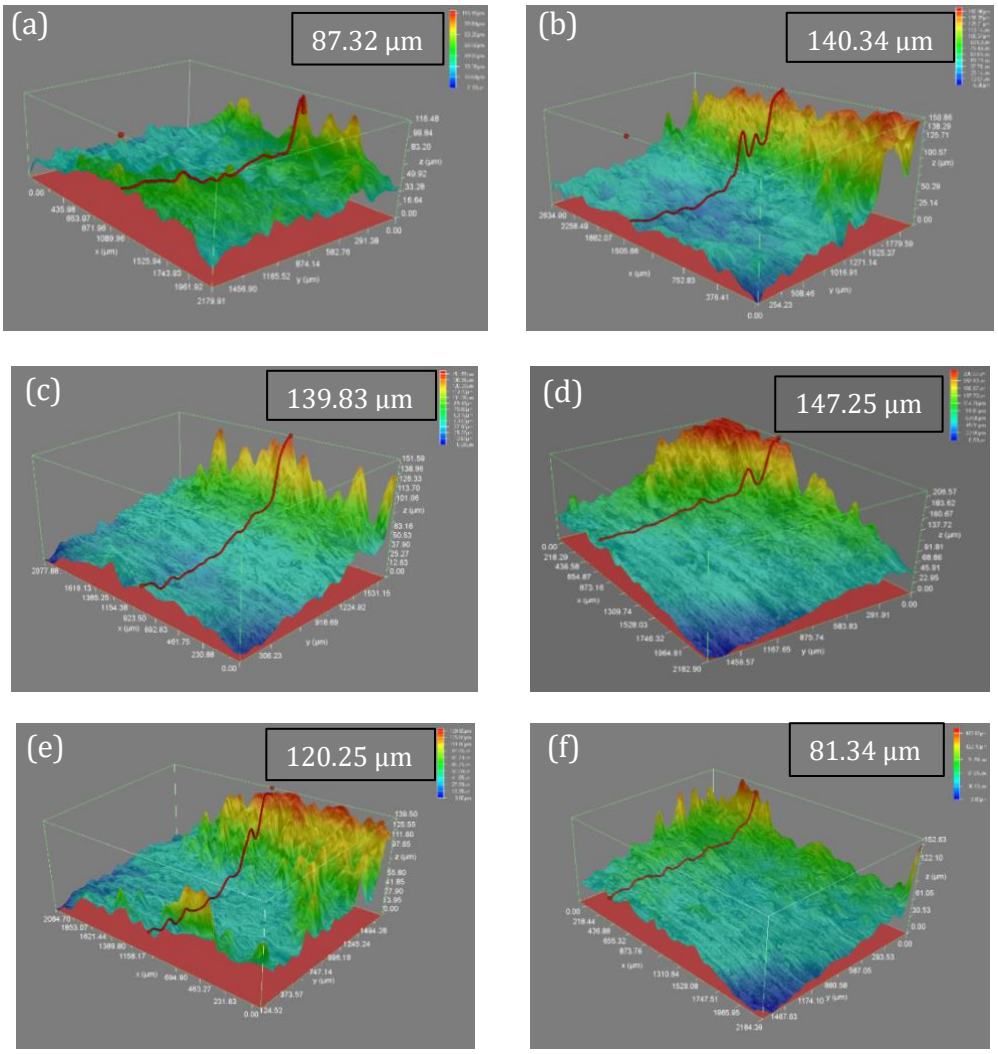

Figure 8: 3D surface topography of TiC nano-composite coating using different TIG process parameters; (a) 120 A 15 PPS, (b) 120 A 20 PPS, (c) 120 A 25 PPS, (d) 140 A 15 PPS, (e) 140 A 20 PPS and (d) 140 A 25 PPS.

Conversely, at arcing currents of 140 A and 15 PPS as shown in Figure 8(d), the wear depth was the highest at 147.25 µm. This increase in wear depth could be attributed to excessive heat input and instability in the coating process, leading to higher material loss and rougher surfaces. Additionally, as the pulse frequencies increased from 20 to 25 PPS (Figures 8e & 8f), the wear depth decreased significantly from 120.25 µm to 81.34 µm, representing a 40.7% decrease. This suggests excellent frictional performance and wear resistance. These findings support from previous study that higher welding currents from 100 A to 150 A resulted in lower wear depth, indicating better wear resistance for enhancing the mechanical properties of AISI 316L using TIG welding. The optimal combination of 150 A current, 16 voltage and 9 L/min gas flow rate produced the smooth surface with the lowest surface roughness at 7.33 µm (Ghumman et al., 2025). The decrease in wear depth, detailed in Table 5, indicates enhanced frictional performance and wear resistance at higher current and pulse frequencies.

Table 5: Wear depth on the wear scars of nano-composite coating under different parameters.

Exp. No.	TIG parameters	Maximum Height (µm)	Minimum Height (µm)	Total Wear Depth (µm)
1	120 A 15 PPS	137.07	49.75	87.32
2	120 A 20 PPS	157.34	17.00	140.34
3	120 A 25 PPS	158.00	18.17	139.83
4	140 A 15 PPS	212.05	64.80	147.25
5	140 A 20 PPS	138.53	21.33	120.25
6	140 A 25 PPS	113.94	32.60	81.34

3.5 Wear Scar of TiC Nano-Composite Coating

The wear scar behavior of the TiC nanocomposite coating on the DSS surfaces was examined using SEM images taken at x100 magnifications, as shown in Figures 9 (a-f). The images demonstrate the formation of wear tracks over the surface of the composite coating layer. At 120 A and 15 PPS (Figure 9a), the wear marks on the surface of the TiC nanocomposite coating shows deep grooves and severe ploughing. These significant material removals and deformations lead to the material being less strong and more prone to faster wear and tears. Next, when the pulse frequency increases to 20 PPS (Figure 9b), it shows that while deep grooves are reduced, severe ploughing is still present. This means that the increased pulse frequency moderates the heat input, making it less intense but still enough to cause significant material displacement, which can affect the surface texture. On the other hand, at 25 PPS as shown in Figure 9(c), the wear scars show the formation of deep grooves and spalling craters. Spalling craters can compromise the protective nature of the coating and expose the underlying material to further wear and corrosion. Additionally, increasing the pulse frequency with an arcing current of 120 A can cause uneven distribution of the TiC nanoparticles, leading to localized areas of weakness that are more susceptible to wear and fracture. Additionally, the black, pore-like feature may result from abrasive wear. During sliding, wear debris can embed into the surface, forming such pores consistent with the severe ploughing observed.

For arcing currents of 140 A and 15 PPS, the wear scars show ploughing, indicating material displacement without severe cracking or grooving, as shown in Figure 9(d). This leads to rough surface textures and increased friction. Moreover, at 20 PPS (Figure 9e), the combination of high current and moderate pulse rate results in spalling craters and deep grooves. The presence of spalling craters suggests that the coating may experience a brittle fracture. Nonetheless, the best

parameter set is 140 A and 25 PPS, as this produces wear scars with only shallow grooves and mild ploughing, as presented in Figure 9(f). The combination of high current and high pulse frequency optimizes the presence of TiC nanocomposite coating on the surface of DSS, indicating a robust coating that effectively resists deformation and wear, leading to a lower coefficient of friction and improved wear resistance.

Therefore, higher currents and pulse frequencies result in less severe wear, while the lowest current causes more pronounced wear features like deep grooves, severe ploughing, and spalling craters. The wear mechanism shows that ploughing and adhesive wear are the key mechanisms of this sample. The results obtained agreed with previous work carried out by Debta & Masanta., (2023), studied a TiC-Co-nY_2O_3 clad layer deposited on a Ti-6Al-4V alloy plate through TIG cladding. It revealed that cladding without nano-Y_2O_3 exhibited the highest worn-out area, whereas cladding with 2 wt% Y_2O_3 showed the least worn area. TiC-Co cladding had a larger worn surface due to its lower wear resistance compared to nano-Y_2O_3 content claddings. The worn surfaces displayed ploughing furrows, minor scratches, and delaminated layers, confirming lower resistance against plastic deformation. Additionally, Paijan et al., (2024) also studied the deposition of SiC coating with the TIG torch method. The Taguchi method was used to optimize the TIG torch melting process of DSS in order to improve wear properties. The results showed that the SiC particles embedded in the DSS surface were strongly bonded to the substrate material, which significantly improved wear resistance. As a result, the hard surface layer formed in the SiC-DSS reinforced surface demonstrated increased durability and did not easily detach during reciprocating wear tests. Furthermore, the best sample produced during the experiments showed smooth striation conditions, indicating superior performance when compared to the other tested samples.

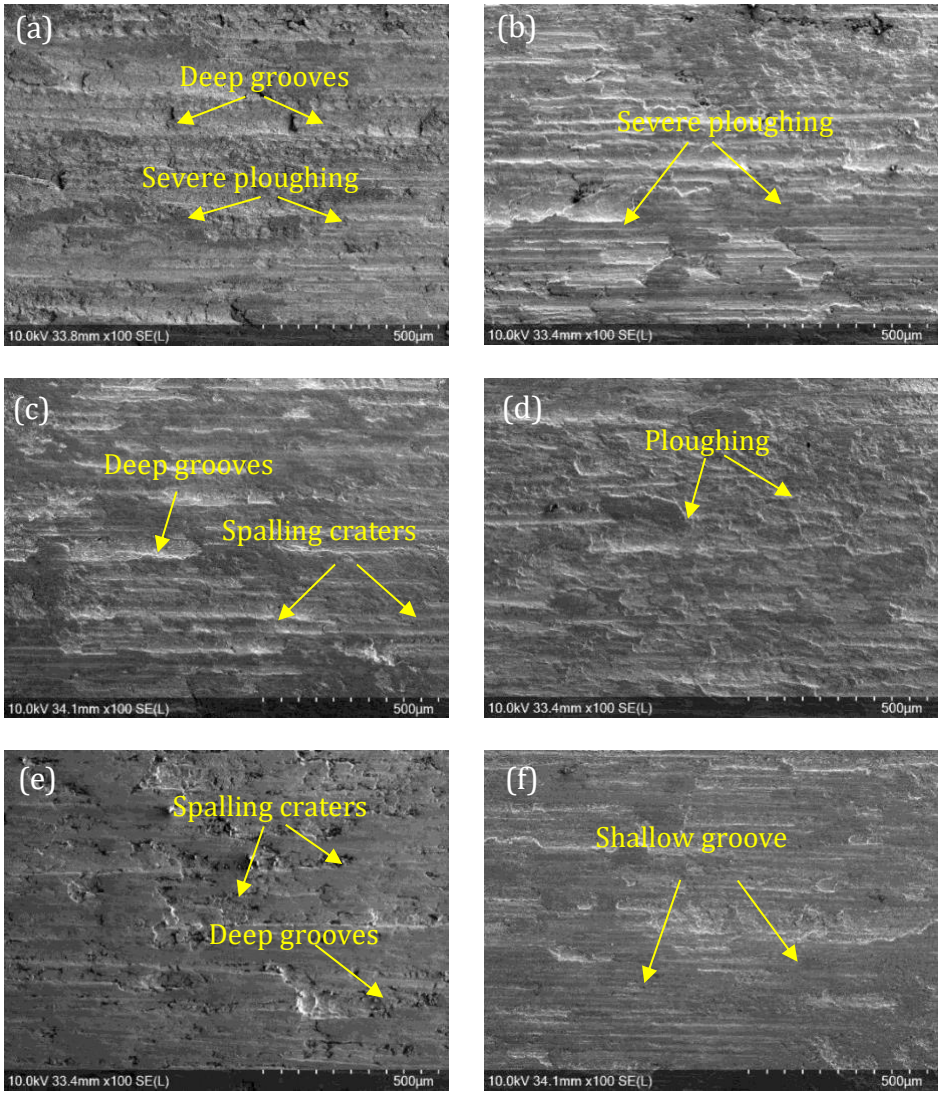

Figure 9: Wear Scar of TiC nano-composite coating using different TIG process parameters; (a) 120 A 15 PPS, (b) 120 A 20 PPS, (c) 120 A 25 PPS, (d) 140 A 15 PPS, (e) 140 A 20 PPS and (d) 140 A 25 PPS.

CONCLUSIONS

This study highlights the surface modification of DSS through the deposition of 10 nm TiC nanoparticles using the TIG melting technique, which revealed significant improvements in the material's wear resistance. Key findings include:

(a) The maximum coating thickness of 900 µm layer was achieved at 140 A and 25 PPS due to optimal energy input for uniform deposition, while lower currents of 120 A resulted in thinner coating layer ranging between 320 µm and 500 µm.

(b) The highest hardness value of 394.3 Hv was observed at 140 A and 25 PPS, where balanced energy input ensured good ceramic particles bonding and high population of TiC nanoparticles in the composite coating layer. Higher currents and pulse frequencies improved the dispersion and melting of TiC particles, improving their deposition and penetration into the DSS matrix surface and influencing hardness and wear behavior.
(c) The lowest coefficient of friction of 0.08 was obtained in the sample fabricated using 140 A and 25 PPS, producing smooth coating and less friction with lesser wear penetration of 81.34 μm and mild ploughing worn surface.

Overall, the best tribological performance was observed at 140 A and 25 PPS, making these conditions ideal for tribological applications. This study highlights the effectiveness of TiC nanoparticles composite coating on DSS using TIG torch melting for enhancing hardness and wear properties emphasizing the need for optimizing processing parameters thereby contributing to the advancements in wear applications.

ACKNOWLEDGEMENT

The financial support for this research was provided by FRGS/1/2023/TK10/UTEM/02/1 and FRGS/1/2023/FTKIP/F00554. Authors also are grateful to Universiti Teknikal Malaysia Melaka for the support that made this study possible.

REFERENCES

Ardeshir, M., Yousefpour, M., Sadegh, N. S. M., & Bozorg, M. (2024). Microstructure and corrosion resistance of high entropy alloy (AlNiCoCrFe) coatings prepared by TIG process. Heliyon, 10(24).

Azevedo, S. C., & Resende, A. A. (2021). Effect of angle, distance between electrodes and TIG current on the weld bead geometry in TIG-MIG/MAG welding process. International Journal of Advanced Manufacturing Technology, 114(5–6), 1505–1515.

Chi, Y., Gong, G., Zhao, L., Yu, H., Tian, H., Du, X., & Chen, C. (2021). In-situ TiB_2-TiC reinforced Fe-Al composite coating on 6061 aluminum alloy by laser surface modification. Journal of Materials Processing Technology, 294.

Debta, M. K., & Masanta, M. (2023). Effect of nano-Y_2O_3 on the microstructure and wear behaviour of TIG cladded TiC-Co-nY_2O_3 coating. International Journal of Refractory Metals and Hard Materials, 111.

Ghumman, K. Z., Ali, S., Khan, N. B., Khan, M. I., Ali, H. T., & Ashurov, M. (2025). Optimization of TIG welding parameters for enhanced mechanical properties in AISI 316L stainless steel welds. The International Journal of Advanced Manufacturing Technology, 136(1), 353–365.

Paijan, L. H., Maleque, M. A., Adeyemi, B. K., Mamat, F. M., & Hussein, I. S. N. (2023). Influence of ceramic particles size on the incorporation of SiC into stainless steel material using 480 J/mm heat input for tribological applications. In Jurnal Tribologi (Vol. 37).

Paijan, L. H., Maleque, M. A., Bakar, A. H. M., Ali, B. M., Mamat, F. M., Osman, H. M., & Asari, M. R. (2022). Taguchi optimization of hardness properties and study the effect on microstructural features of SiC reinforced composite coating duplex stainless steel. Malaysian Journal of Microscopy, 18(2), 189–200.

Paijan, L. H., & Maleque, A. (2018). Tribological properties of surface coated duplex stainless steel containing SiC ceramic particles. In Jurnal Tribologi (Vol. 18).

Paijan, L. H., Maleque, M. A., Rosli, Z. M., Abdollah, M. F., Mamat, M. F., & Nazrin, A. (2024). Taguchi Optimization of Wear Properties of Duplex Stainless Steel Reinforced Surface with Silicon Carbide Using TIG Torch Melting.

Islam, T., & Rashed, H. M. M. A. (2019). Classification and application of plain carbon steels. In Reference Module in Materials Science and Materials Engineering. Elsevier.

Kısasöz, A., Karaaslan, A., & Kisasoz, A. (2017). Variation of microstructure and mechanical properties of 2205 duplex stainless steel for solution treatment at 1150˚C. International Conference on Engineering Technology and Innovation.

Kumar, A., & Das, A. K. (2021). Evolution of microstructure and mechanical properties of Co-SiC tungsten inert gas cladded coating on 304 stainless steels. Engineering Science and Technology, an International Journal, 24(3).

Maleque, M. A., Paijan, L. H., Bello, K., Azwan, M., & Rahman, M. M. (2018). Tribological properties of surface modified Ti-6Al-4V alloy under lubricated condition using Taguchi approach. In Jurnal Tribologi (Vol. 17).

Maleque, M. A., & Afiq, M. (2018). Melting of SiC powders preplaced duplex stainless steel using TIG welding. IOP Conference Series: Materials Science and Engineering, 290(1).

Maleque, M. A., Idriss, A. N. M., Naping, R., Rahman, M. M., & Efeoglu, I. (2024). The Influence of TiC Dispersion and Density on the Microstructural Features and Microhardness Fused by TIG Arc Process. Journal of Advanced Research in Applied Mechanics, 114(1), 33–42.

Paraye, N. K., Neog, S. P., Ghosh, P. K., & Das, S. (2021). Surface modification of AISI 8620 steel by in-situ grown TiC particle using TIG arcing. Surface and Coatings Technology, 405.

Shi, Z. P., Wang, Z. Bin, Wang, J. Q., Qiao, Y. X., Chen, H. N., Xiong, T. Y., & Zheng, Y. G. (2020). Effect of Ni interlayer on cavitation erosion resistance of NiTi cladding by tungsten inert gas (TIG) surfacing process. Acta Metallurgica Sinica (English Letters), 33(3), 415–424.

Sun, Y., Sun, J., Jin, J., & Xu, H. (2022). Effect of TiC on microstructure and properties of wear-resistant Mo_2FeB_2 claddings. Materials, 15(13).